Application of the Multilevel Single-Linkage Method to One-Dimensional Electromagnetic Inverse Scattering Problem

Mansor Nakhkash, *Member, IEEE*, Yi Huang, *Member, IEEE*, and Michael T. C. Fang

***Abstract*—An inverse scattering method for the reconstruction of the permittivity and conductivity profiles of a multilayered medium and for that of the impedance profile of a nonuniform transmission line is proposed. The inversion is based on the global minimization of an objective function by the multilevel single-linkage method. The objective function is defined as the mean-square error between the measured data and the data obtained from the solution of the forward problem. An exact formulation for the gradient of the objective function in closed form is derived. The necessary condition for the unique solution of the inverse problem of a nonuniform transmission line is discussed. Reconstruction examples using both experimental and noisy synthetic data are presented.**

***Index Terms*—Inverse scattering, nonhomogeneous media.**

I. Introduction

The one-dimensional (1-D) inverse scattering problem is to reconstruct the material parameters of layered media from the so-called scattering data, e.g., reflection coefficients measured at different frequencies and/or at different incident angles. The reconstruction of the permittivity and conductivity profiles of a multilayered medium and the identification of the impedance profile of a nonuniform transmission line, are the examples of typical 1-D inverse scattering problems. One-dimensional inversion methods can be divided into two categories [1]. The first category includes all direct inversion methods such as the layer stripping method [2]–[4]. The second comprises the so-called model-based inversion methods. When the scattering data is incomplete and contaminated with noise, the performance of the second category is superior to the first. Much attention has therefore been paid to the model-based inversion approach.

Model-based inversion methods rely on an optimization procedure in which the profile of a medium is reconstructed by optimizing a suitable objective function. The value of this function indicates the closeness between the observed (measured) data and the synthetic data that is generated by solving the forward scattering problem. In general, because the forward model is nonlinear, the resulting objective function may have several optima. The model-based inversion methods only yield the correct results if they converge to the global optimum of the objective function.

Local optimization methods such as the conjugate gradient method have often been used for 1-D inverse scattering problems [5]–[7]. To ensure the convergency of a local optimization method to the global optimum, *a priori* information must be incorporated in the definition of the objective function as well as in the selection of the initial profile. However, there is no certainty that the method converges to the true solution, which corresponds to the global optimum. One way to overcome this problem is to apply global optimization methods, such as simulated annealing (SA) [8], and genetic algorithms (GA) [1].

SA is based on the analogy between the physical annealing process of solids and the problem of finding the minimum of an objective function [9]. In SA, a control parameter known as the temperature is lowered slowly while at each temperature several values for the objective function are experienced. As cooling proceeds, the variation domain of the function is reduced and becomes restricted to a point (minimum point) at temperature zero. GA optimize a function using processes inspired from the mechanics of natural selection and genetics (e.g., crossover and mutation) [10]. The optimization is accomplished by evolving a population of candidate solutions and improving incrementally the individuals forming the population.

The main drawbacks of SA and GA are that they are not efficient in terms of computation time and are not sufficiently accurate in locating the exact solution. On the other hand, the multilevel single-linkage method (MLSL), which incorporates a local optimization method into the global search [11]–[13], offers efficiency and accuracy. A comparison between GA and MLSL has been performed by Renders and Flasse [14]. They have proposed a hybrid version of genetic algorithms combining principles from GA and local gradient search techniques to reduce the computing time and to improve the accuracy of GA. The conclusion was that the hybrid method is superior to the standard GA but, overall, it produces poorer results than those of MLSL. In addition, the convergence of GA and its variants to the global optimum is only guaranteed in a weak probabilistic sense, whereas there exists a probabilistic guarantee that the MLSL finds the global optimum of a function within a finite number of local searches. The MLSL also offers a significant improvement in accuracy and efficiency over SA [15]. The limitation of the MLSL is that the method

Manuscript received March 26, 1998; revised August 16, 1999. This work was supported by the Leverhulme Trust, U.K.

The authors are with the Department of Electrical Engineering and Electronics, University of Liverpool, Liverpool, L69 3BX, U.K.

Publisher Item Identifier S 0018-926X(99)09944-5.

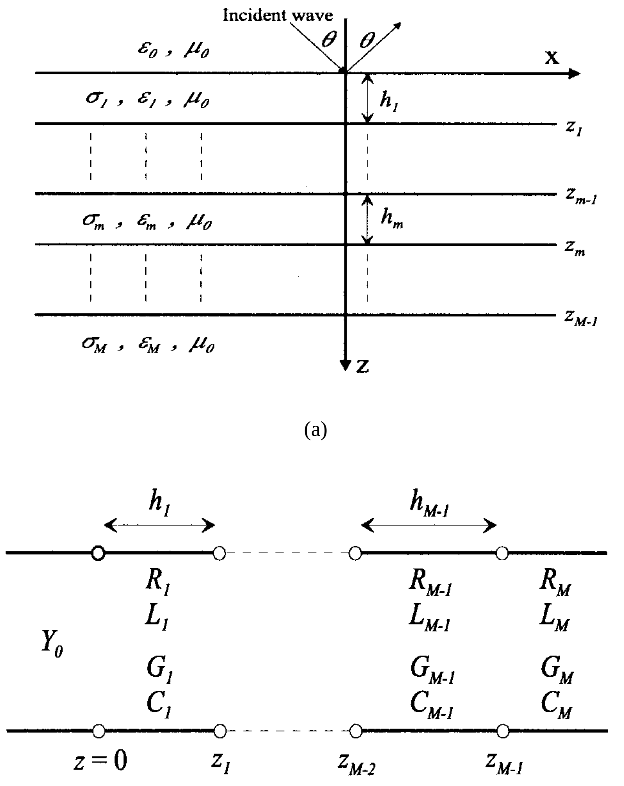

(b)

Fig. 1. (a) The structure of an M-layer medium. (b) The structure of a nonuniform transmission line.

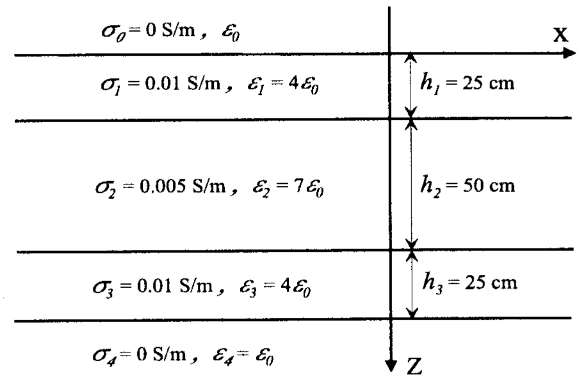

Fig. 2. A three-layer slab placed in free-space.

is based on the assumption that the function and its gradient are continuous. The advantages of SA and the standard GA are that they require only the value of the objective function and they are simple to implement.

In this paper, a 1-D inverse scattering method based on the MLSL is used to reconstruct the permittivity and conductivity profiles of a multilayered medium. The method is also applied to find the parameters of a nonuniform transmission line. The MLSL is employed to minimize the mean-square error (MSE) function, which is obtained from the difference between the measured reflection coefficients and those calculated from the forward model. The forward model for multilayered media and the transmission line can be formulated in a closed-form [16]. In the present paper, the gradient of the objective function is derived analytically. This greatly increases the efficiency of the inversion method. There is no need to specify the initial profile for the proposed method, although the bounds of the parameters have to be specified. Thus, any prior knowledge of the parameters can be used to narrow the parameter bounds. For multilayered media, the inversion method offers simultaneous reconstruction of the permittivity and conductivity profiles from the reflection coefficient data of a TEM plane wave at a set of discrete frequencies. The necessary condition for reconstructing uniquely the parameters of a nonuniform transmission line from the reflection coefficient data will also be discussed.

Several reconstruction examples are used to demonstrate the performance of the proposed 1-D inversion method. In the case of multilayered media the observed data is synthetic, i.e., the simulated reflection coefficient. Gaussian noise is added to this data to simulate practical applications. For the nonuniform transmission line, both experimental and noisy synthetic data are used. The experimental reflection coefficients are measured by using an HP-8753B network analyzer.

II. Formulation of the Forward Problem

The derivation of the reflection coefficient for multilayered media and for a nonuniform transmission line is well known, e.g., [16]. For completeness and for ease of later discussion, the expressions necessary for the solution of the forward problem are given below.

A. Multilayered Medium

The geometry of the problem is illustrated in Fig. 1(a) where a TE wave is incident on the first interface at $z = 0$. The multilayered medium consists of M homogeneous layers. The mth layer is characterized by conductivity σ_m, permittivity ϵ_m, permeability μ_0 and thickness h_m. Suppose that the incident TE plane wave has a y-component electric field with an incident angle θ relative to z direction and has time factor $\exp(j\omega t)$, where ω is the angular frequency. The reflection coefficient at $z = 0$ is given by

$$H(\omega) = \frac{Y_0 - W_1}{Y_0 + W_1}. \tag{1}$$

W_1 can be derived from

$$W_m = Y_m \frac{W_{m+1} + Y_m \tanh u_m h_m}{Y_m + W_{m+1} \tanh u_m h_m} \tag{2}$$

where $m = 1, 2, \cdots, M-1$, and W_M is given by

$$W_M = Y_M. \tag{3}$$

Y_m, the intrinsic admittance of the mth layer, and u_m are given by

$$Y_m = \frac{u_m}{j\omega\mu_0} \tag{4}$$

$$u_m = \left[\gamma_m^2 - \gamma_0^2 \sin^2\theta\right]^{1/2} \tag{5}$$

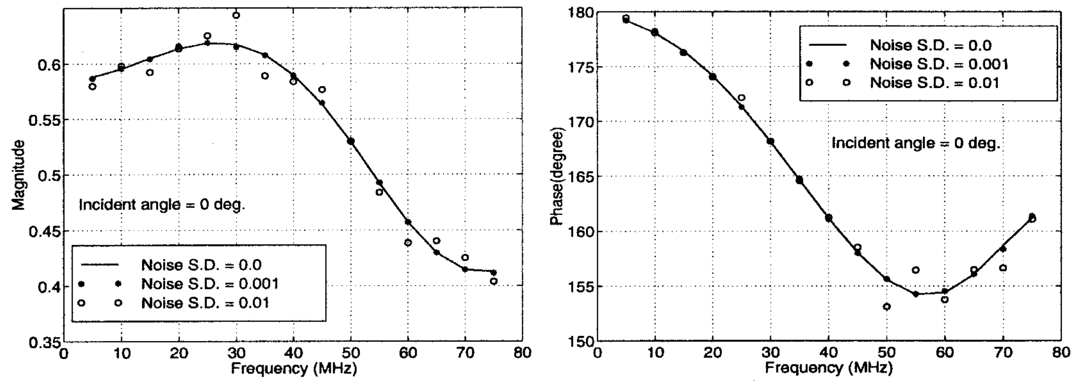

(a)

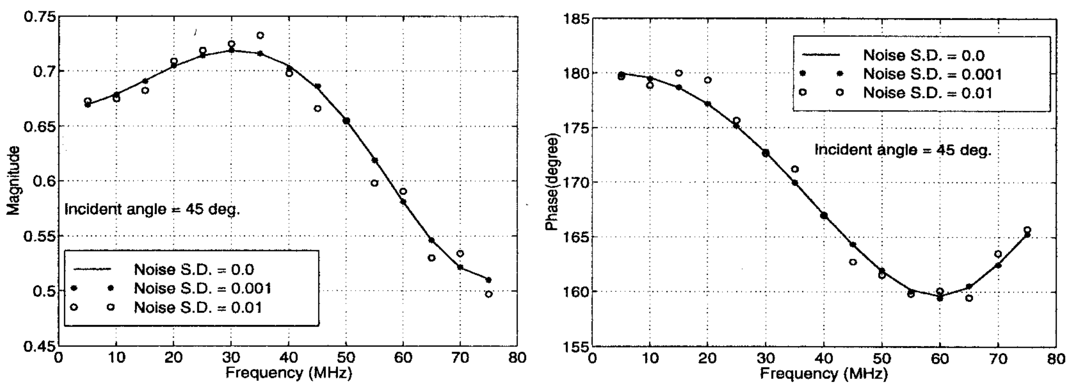

(b)

Fig. 3. Synthetic data for the reflection coefficients of the three-layer slab obtained for a TE wave incidence at 15 frequencies equally spaced in the interval [5 MHz, 75 MHz]. (a) Incident angle $\theta = 0°$. (b) Incident angle $\theta = 45°$.

where γ_m, the propagation constant of the mth layer, is equal to

$$\gamma_m = [j\mu_0\sigma_m\omega - \mu_0\epsilon_m\omega^2]^{1/2}. \quad (6)$$

A. Nonuniform Transmission Line

Fig. 1(b) shows a nonuniform transmission line with M uniform sections. R_m, L_m, C_m, and G_m are, respectively, the series resistance, series inductance, shunt capacitance, and shunt conductance per unit length; h_m denotes the length of the mth section. The nonuniform line is excited at $z = 0$ from a uniform transmission line with a characteristic admittance Y_0. There is a direct analogy between a multilayered medium and a nonuniform transmission line [16]. The expressions derived in the previous subsection are equally applicable here. In addition, $u_m = \gamma_m$ (i.e., $\theta = 0°$) and the expression for Y_m [17] is changed to

$$Y_m = \frac{u_m}{R_m + j\omega L_m} \quad (7)$$

where Y_m is the characteristic admittance of the mth section. The propagation constant γ_m is given by

$$\gamma_m = [(R_m + j\omega L_m)(G_m + j\omega C_m)]^{1/2}. \quad (8)$$

III. Inverse Scattering Method

Consider $r_1, r_2, \cdots, r_N$ are the measured reflection coefficients at a number of frequencies. For a multilayered medium, they can be measured at a number of incident angles as well. Furthermore, consider $\mathbf{x}$ as a point in a multidimensional space with the dimension given by all constitutive parameters defining a layered medium or a nonuniform transmission line, e.g., for a multilayer medium, this point can be represented as

$$\begin{aligned}\mathbf{x} &= (x_1, x_2, x_3, \cdots, x_{K-1}, x_K)\\ &= (\sigma_1, \epsilon_1, h_1, \cdots, \sigma_M, \epsilon_M)\end{aligned} \quad (9)$$

where $K = 3M - 1$. The objective function for the inversion method is defined as follows:

$$f(\mathbf{x}) = \frac{1}{2N}\sum_{n=1}^{N} |H_n(\mathbf{x}) - r_n|^2 \quad (10)$$

where $H_n(\mathbf{x})$ denotes the reflection coefficient obtained from the forward model under the same conditions as the measured data r_n. The actual constitutive parameters are found by minimization of the function $f(\mathbf{x})$. A global optimization method should be used for $f(\mathbf{x})$, which may have several minima. For the present investigation, the MLSL method is adopted due to its efficiency in comparison with other methods [9], [10], [14], [18], [19].

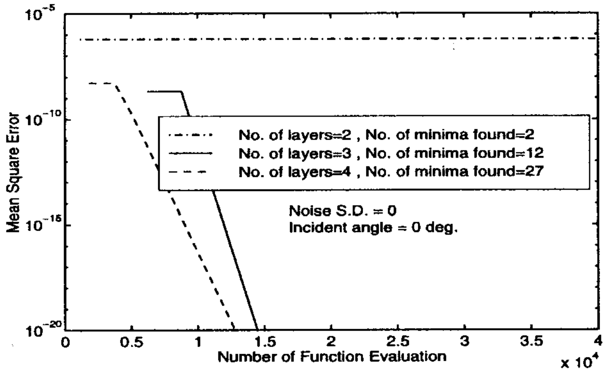

Fig. 4. Illustration of the performance of the MLSL method in minimizing the objective function for the three-layer slab. The number of layers assumed is two, three, and four. The observed data at $\theta = 0°$ is free of noise.

Because of the nonlinearity of the forward model together with the inadequacy of the measured data, inverse scattering problems are often ill-posed. An ill-posed problem can be converted to a well-posed one by introducing the bounds on the parameters on physical grounds [1]. The global minimum is therefore found within the range of parameters specified by

For a multilayered medium:

$$\sigma_m^{\rm Min} \le \sigma_m \le \sigma_m^{\rm Max}, \quad \epsilon_m^{\rm Min} \le \epsilon_m \le \epsilon_m^{\rm Max}$$
$$h_m^{\rm Min} \le h_m \le h_m^{\rm Max}, \quad m = 1, \cdots, M.$$

For a nonuniform transmission line:

$$R_m^{\rm Min} \le R_m \le R_m^{\rm Max}, \quad L_m^{\rm Min} \le L_m \le L_m^{\rm Max}$$
$$G_m^{\rm Min} \le G_m \le G_m^{\rm Max}, \quad C_m^{\rm Min} \le C_m \le C_m^{\rm Max}$$
$$h_m^{\rm Min} \le h_m \le h_m^{\rm Max}, \quad m = 1, \cdots, M. \tag{11}$$

It should be noted that the inverse method cannot reconstruct the five parameters defining a section of a nonuniform transmission line. The necessary condition which must be satisfied in order to uniquely reconstruct the profile of a nonuniform transmission line is discussed in Section III-C below. A brief account of the algorithm associated with the MLSL method and the derivation of the gradient of the objective function required by the MLSL method are given, respectively, in Sections III-A and B.

A. The Multilevel Single-Linkage Method

The MLSL method is used to search the global minimum of the objective function $f(\mathbf{x})$ in a feasible region S defined by

$$S = \{\mathbf{x} \mid l_i \le x_i \le u_i, \ i = 1, \cdots, K\} \tag{12}$$

where l_i and u_i are respectively the lower and upper bounds of the parameter x_i.

The MLSL method is a stochastic iterative algorithm, which combines random search with a local optimization method. The kth iteration of the algorithm outlined by Byrd *et al.* [13] is as follows.

1) Generate P sample points drawn from a uniform distribution over S, and calculate the corresponding functional values at these points. Add P points to the (initially empty) set of sample points.

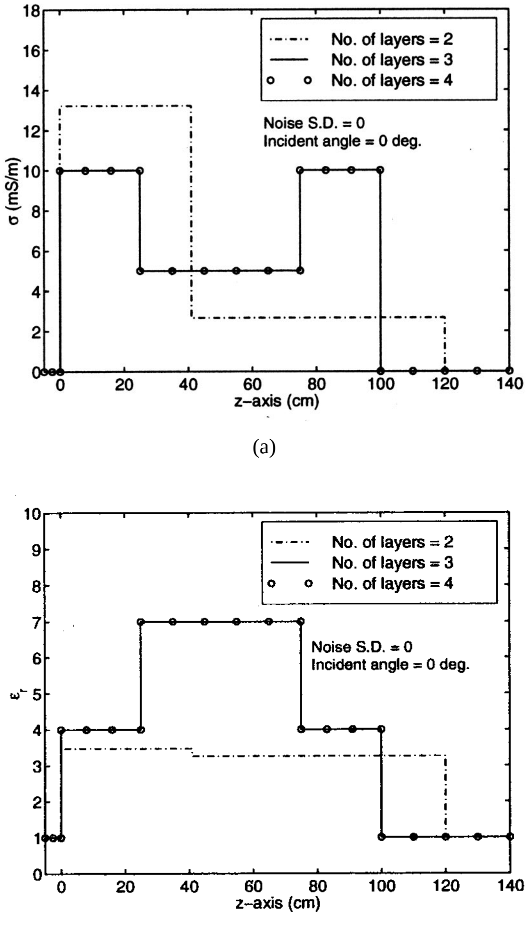

Fig. 5. (a) The conductivity and (b) permittivity profile reconstructed from normal incidence, noise-free data. The three-layer structure is found by the algorithm.

2) Determine a set of the reduced sample points by taking the ξkP points with the smallest function values, where ξ is any fixed number in (0, 1].
3) Select start points from the reduced sample points for local searches. The selection procedure will be discussed later.
4) Perform local minimizations from the selected start points.
5) If the stopping rule is satisfied, the lowest local minimum is taken as the global minimum, otherwise go to Step 1).

In Step 3), at the kth iteration, each reduced sample point $\mathbf{x}$ is selected as a start point for a local minimization provided that the start point has not been used at a previous iteration and that there is no sample point $\mathbf{y}$ within the critical distance $d(k)$ of $\mathbf{x}$ with $f(\mathbf{y}) < f(\mathbf{x})$. The critical distance is given by [12]

$$d(k) = \pi^{-1/2}\left[\Gamma\left(1 + \frac{K}{2}\right)\Psi(S)\rho\frac{\log kP}{kP}\right]^{1/K} \tag{13}$$

where Γ denotes the gamma function, $\Psi(S)$ denotes the Lebesque measure of S and ρ is a positive constant. Rinnooy Kan and Timmer [12] have proven that when $\rho > 0$, all local minima of $f(\mathbf{x})$ will be found within a finite number

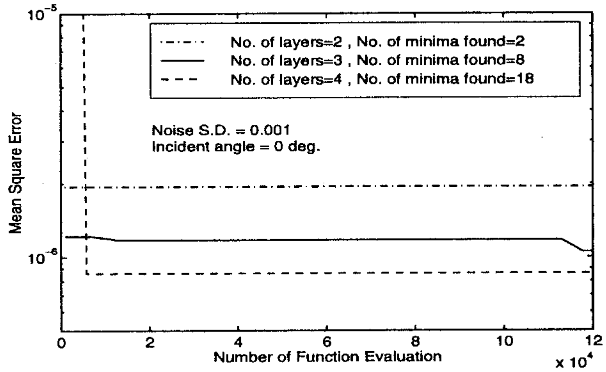

Fig. 6. The objective function versus the number of function evaluations when the observed data at normal incidence is corrupted by a Gaussian noise with $\bar{\sigma} = 10^{-3}$.

of iterations with probability one. Moreover, when $\rho > 4$, the total number of local searches started by the MLSL method will be finite with probability one even if the sampling continues forever. ρ is set to four in our reconstruction examples.

A Bayesian stopping rule is applied in Step 5). Let w denote the number of local minima found after k iterations. A Bayesian estimate of the total number of local minima is given by

$$\frac{w(\xi kP - 1)}{\xi kP - w - 2}. \tag{14}$$

Moreover, a Bayesian estimate of the portion of S covered by the regions of attraction of the local minima found so far is given by

$$\frac{(\xi kP - w - 1)(\xi kP + w)}{\xi kP(\xi kP - 1)}. \tag{15}$$

The algorithm is terminated after the kth iteration if the estimate given by (14) is greater than w by less than 0.5 and the estimate given by (15) is greater than a value near but less than 1 such as 0.999.

A modified Newton's method is used for the local minimization. This method requires both the gradient vector and the Hessian matrix (i.e., the second derivatives) of the objective function to find a minimum point. We derive an exact and closed-form expression for the gradient of the objective function in the next subsection. The Hessian matrix is estimated by finite differences within the optimization routine, which is taken from the NAG library [20].

B. The Closed-Form Expression for the Gradient

The derivation of the gradient for multilayered media is considered first. Let x_m be one of the parameters (σ_m, ϵ_m, and h_m) of the mth layer. The derivative of the objective function f given by (10) with respect to x_m can be obtained as

$$\frac{\partial f}{\partial x_m} = \frac{1}{N}\,\mathrm{Re}\left[\sum_{n=1}^{N}(H_n - r_n)^*\frac{\partial H_n}{\partial x_m}\right] \tag{16}$$

where "Re" and "$*$" denote the real part and complex conjugation, respectively. Using (1)–(3), one can derive

$$\frac{\partial H_n}{\partial x_m} = -2\frac{Y_0}{(Y_0 + W_1)^2}V_m^1, \quad m = 1, 2, \cdots, M \tag{17}$$

where $V_m^i = \partial W_i/\partial x_m$. The expression for V_m^i depends on the relation between i and m. If $i < m$, we have

$$V_m^i = \left(\frac{Y_i}{Y_i + W_{i+1}T_i}\right)^2 (1 - (T_i)^2)V_m^{i+1} \tag{18}$$

where $T_i = \tanh u_i h_i$. For the case of $i = m$ and $x_m = \sigma_m$ or ϵ_m, V_m^m is given by

$$V_m^m = \left(T_m[(W_{m+1})^2 + (Y_m)^2 + 2Y_m W_{m+1} T_m]\frac{\partial Y_m}{\partial x_m} + Y_m[(Y_m)^2 - (W_{m+1})^2]\frac{\partial T_m}{\partial x_m}\right)\Big/(Y_m + W_{m+1}T_m)^2. \tag{19}$$

The expression for V_m^m when $x_m = h_m$ is

$$V_m^m = Y_m u_m[1 - (T_m)^2]\frac{(Y_m)^2 - (W_{m+1})^2}{(Y_m + W_{m+1}T_m)^2}. \tag{20}$$

Finally, for the special case of $m = M$, (19) is simplified to

$$V_M^M = \frac{\partial Y_M}{\partial x_M}. \tag{21}$$

$\partial Y_m/\partial x_m$ and $\partial T_m/\partial x_m$ in (19) and (21) for $x_m = \sigma_m$ and ϵ_m are

$$\frac{\partial Y_m}{\partial \sigma_m} = \frac{1}{2u_m}, \quad \frac{\partial T_m}{\partial \sigma_m} = \frac{[1 - (T_m)^2]h_m}{2Y_m} \tag{22}$$

$$\frac{\partial Y_m}{\partial \epsilon_m} = j\omega_n\frac{\partial Y_m}{\partial \sigma_m}, \quad \frac{\partial T_m}{\partial \epsilon_m} = j\omega_n\frac{\partial T_m}{\partial \sigma_m}. \tag{23}$$

Due to the similarity between the formulation of the forward problem for a multilayered medium and that of a nonuniform transmission line, (16)–(21) are applicable to the latter case. In addition, $\partial Y_m/\partial x_m$ and $\partial T_m/\partial x_m$ for $x_m = R_m$, L_m, G_m, and C_m can be written as

$$\frac{\partial Y_m}{\partial R_m} = -\frac{Y_m^2}{2u_m}, \quad \frac{\partial T_m}{\partial R_m} = \frac{Y_m[1 - (T_m)^2]h_m}{2} \tag{24}$$

$$\frac{\partial Y_m}{\partial L_m} = j\omega_n\frac{\partial Y_m}{\partial R_m}, \quad \frac{\partial T_m}{\partial L_m} = j\omega_n\frac{\partial T_m}{\partial R_m} \tag{25}$$

$$\frac{\partial Y_m}{\partial G_m} = \frac{1}{2u_m}, \quad \frac{\partial T_m}{\partial G_m} = \frac{[1 - (T_m)^2]h_m}{2Y_m} \tag{26}$$

$$\frac{\partial Y_m}{\partial C_m} = j\omega_n\frac{\partial Y_m}{\partial G_m}, \quad \frac{\partial T_m}{\partial C_m} = j\omega_n\frac{\partial T_m}{\partial G_m} \tag{27}$$

where use has been made of (7) and (8).

It is noteworthy that with regard to the recursive equation (18), the computation time for calculating the gradient is in proportion to that needed for calculating the objective function itself. This greatly improves the efficiency of the optimization procedure.

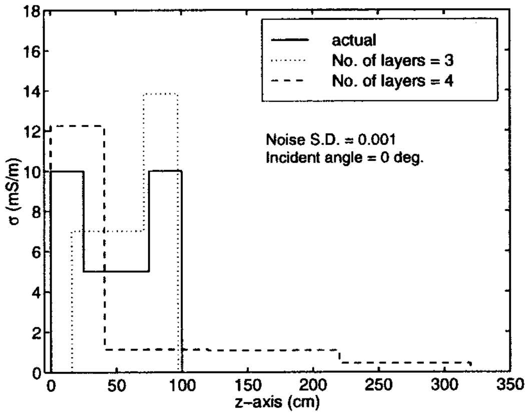

(a)

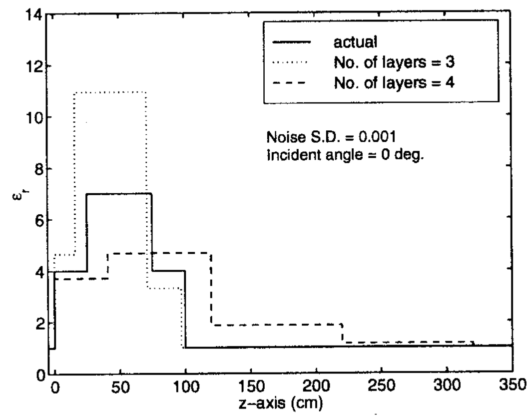

(b)

Fig. 7. Influence of noise on the reconstructed profile.

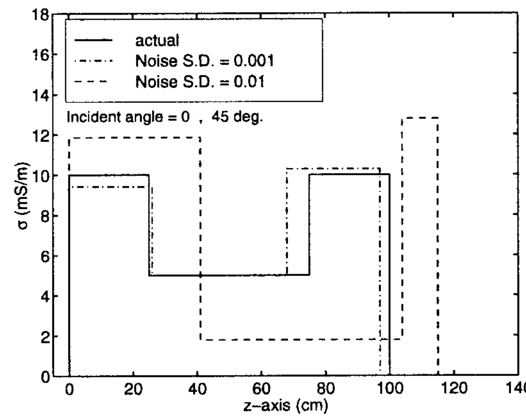

(a)

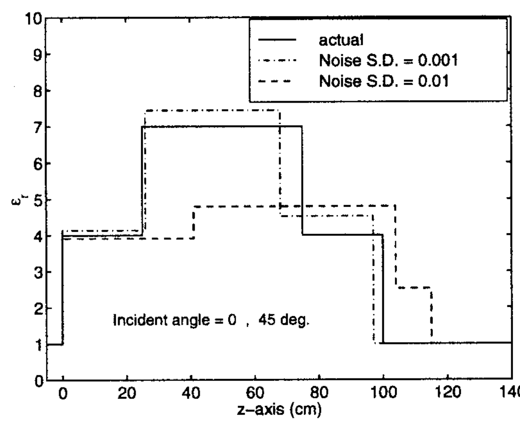

(b)

Fig. 8. Illustration of the improvement of the reconstructed profile for three-layer structure using more observed data. The results are based on the observed data at 15 frequencies and two incident angles (0° and 45°).

C. Necessary Condition for the Unique Reconstruction of the Parameters of a Nonuniform Transmission Line

It is not possible to uniquely reconstruct all five parameters defining a section of a nonuniform transmission line. This is because the reflection coefficient of a nonuniform transmission line depends on these parameters only through T_m and Y_m. Manipulating (7), T_m can be written as

$$T_m = \tanh[(R_m + j\omega L_m)h_m Y_m]. \tag{28}$$

With the known values of Y_m and T_m, we can derive $(R_m + j\omega L_m)h_m$ from the above equation. The value of $(G_m + j\omega C_m)h_m$ is then calculated from Y_m by noting

$$Y_m = \left[\frac{G_m + j\omega C_m}{R_m + j\omega L_m}\right]^{1/2}. \tag{29}$$

Thus, four relations can be derived from the real and imaginary parts of the two complex equations (28) and (29)

$$\begin{cases} R_m h_m = a_R \\ L_m h_m = a_L/\omega \\ G_m h_m = a_G \\ C_m h_m = a_C/\omega. \end{cases} \tag{30}$$

One of the five parameters must be known in order to reconstruct a section of a nonuniform transmission line. Note that the two terms a_L/ω and a_C/ω in (30) are frequency independent. Therefore, the five parameters cannot be calculated by taking into account the value of Y_m and T_m at several frequencies. In practice, R_m and G_m are often negligible. The four conditions are therefore reduced to two. Thus, one of the remaining three parameters must be assumed known. This additional condition is known as the necessary condition for the inverse problem of a nonuniform transmission line. In a similar manner, it can be shown that this condition is valid even if both transmission and reflection data are available.

IV. RECONSTRUCTION EXAMPLES

This section is devoted to three reconstruction examples to demonstrate the proposed inversion method.

A. General Considerations

In the usual description of the inversion method, it is assumed that the number of layers is known, which is often *a priori* information in some applications. However, if the number of layers is unknown, to find the structure of a

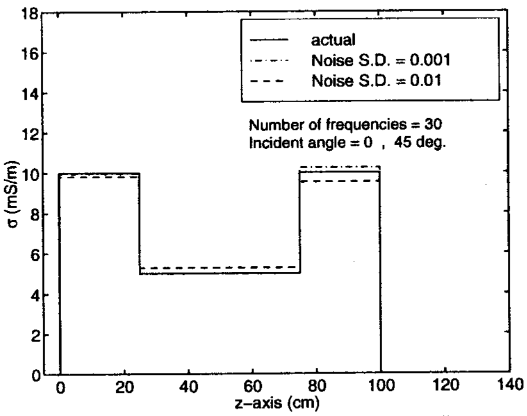

(a)

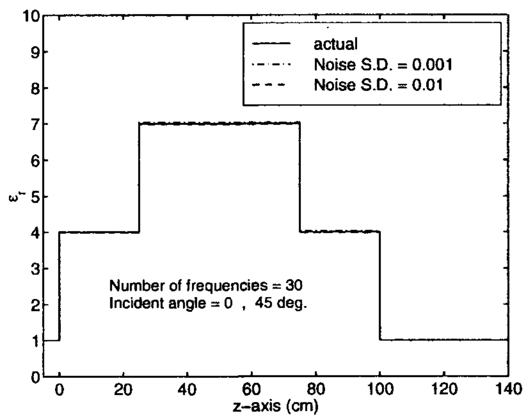

(b)

Fig. 9. (a) The conductivity and (b) permittivity profiles of the three-layer slab reconstructed from the reflection coefficients obtained at two incident angles (0° and 45°) and at 30 frequencies over the range of [5 MHz, 150 MHz] with linear spacing.

medium, the present method employs a procedure which makes use of the inversion method iteratively. At the kth iteration of this procedure, while the medium is considered to consists of k layers, the constitutive parameters of the medium are reconstructed by the inversion method. The resultant MSE, $\tilde{f}_k$, which is viewed as the value of the objective function at its global minimum, is compared with the one from the $(k-1)$th iteration $(\tilde{f}_{k-1})$. If they are sufficiently close, two cases may arise: one is that the parameters of two adjacent layers are matched (i.e., $\sigma_m = \sigma_{m-1}$ and $\epsilon_m = \epsilon_{m-1}$) and the other is that the thickness of a layer converges to zero. For both cases, one layer can be omitted and the reconstructed profile for k-layer medium is the same as that for $(k-1)$-layer medium. This would happen for $k = M+1$, where M is the actual number of layers. When the observed data is free of noise, the value of the objective function at its global minimum for M-layer and $(M+1)$-layer mediums are equal (i.e., $\tilde{f}_M = \tilde{f}_{M+1}$). For the case where the data is corrupted by noise, we generally have $\tilde{f}_{M+1} \leq \tilde{f}_M$. Consequently, the iterative procedure at

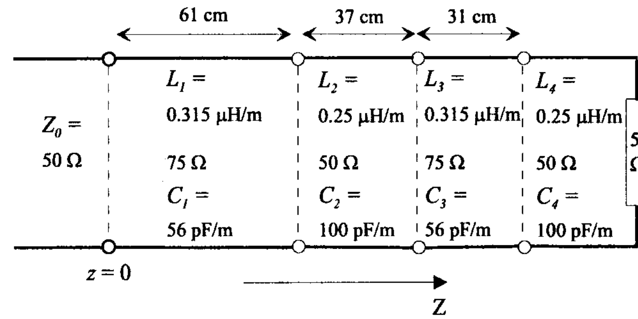

Fig. 10. A nonuniform transmission line.

iteration k is terminated if

$$|\tilde{f}_k - \tilde{f}_{k-1}| \leq \eta \tilde{f}_k \tag{31}$$

where η is a small value less than one. Otherwise, the number of layers is incremented and the process is repeated.

The computational efficiency of global optimization methods is usually measured in terms of the number of evaluations of the objective function. Both the evaluation of the objective function and that of its gradient are required by the MLSL method. In order to estimate the computation cost, the computation time for gradient evaluation is measured as a proportion of that for the function evaluation. For the examples given below, it has been found that the proportional constant is nearly two.

B. Examples

Example 1: This example is the one considered in [5]. The goal is to reconstruct the permittivity and conductivity profiles of a three-layer slab placed in free-space as shown in Fig. 2. The thickness of the whole ensemble together with the permittivity and conductivity of the bottom half-space are assumed known in [5]. In contrast, we only assume that the bottom layer is free-space. The observed data, r_n, are generated by using the equations presented in Section II.

To simulate the presence of the noise in the observed data, Gaussian noise is added. The noise is a complex random variable whose real and imaginary parts are independent Gaussian random variables with zero mean and standard deviation $\bar{\sigma}$.

The parameters of P and ξ in the MLSL method are set to 500 and 0.01, respectively. In addition, the feasible region S is given by

$$0 \leq \sigma_m \leq 0.5 \text{ S/m}, \quad \epsilon_0 \leq \epsilon_m \leq 100\epsilon_0$$
$$0 \leq h_m \leq 100 \text{ cm}, \quad m = 1, 2, 3.$$

The above bounds on permittivity and conductivity are sufficiently wide that they cover the permittivity and conductivity of most materials, which may be found in an environment.

As shown in Fig. 3, the reflection coefficients are obtained for a TE wave incidence at 15 frequencies equally spaced in the interval [5 MHz, 75 MHz] and at two incident angles $\theta = 0°$ and $45°$. Gaussian noise with different standard deviations is introduced to simulate the effect of noise.

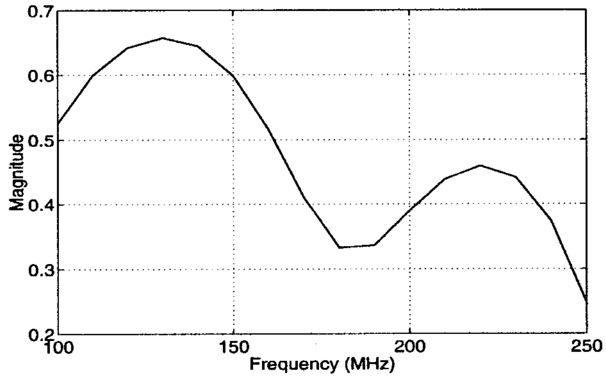

(a)

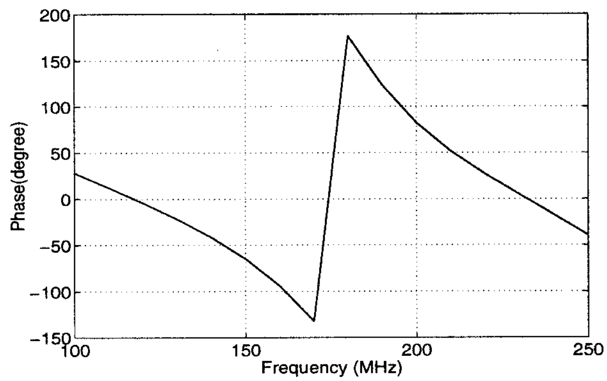

(b)

Fig. 11. The reflection coefficients of the transmission line shown in Fig. 10. The data is measured by an HP-8753B network analyzer at 16 frequencies equally spaced in the interval [100 MHz, 250 MHz].

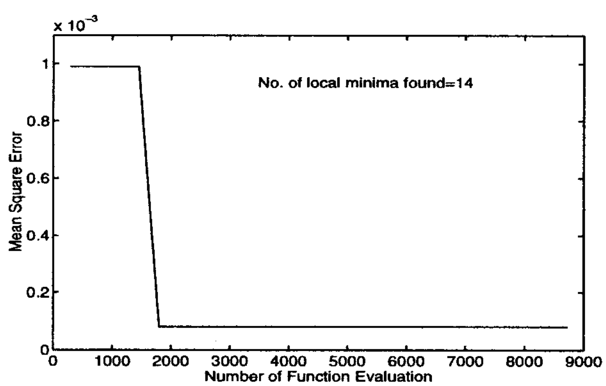

Fig. 12. Illustration of the performance of the MLSL method in minimizing the objective function for the transmission line shown in Fig. 10.

The profile is first reconstructed from noise-free data at an incident angle $\theta = 0°$. Fig. 4 illustrates that how the objective function is reduced by the MLSL method under the assumptions that the number of layers is two, three, and four. The number of minima for each layer structure is also given. The conductivity and permittivity profiles derived from the inversion method are shown in Fig. 5. Three features

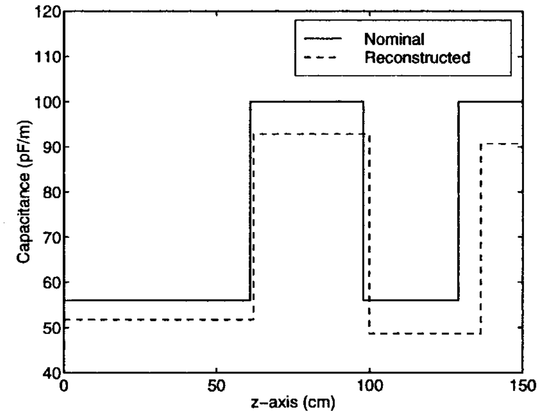

(a)

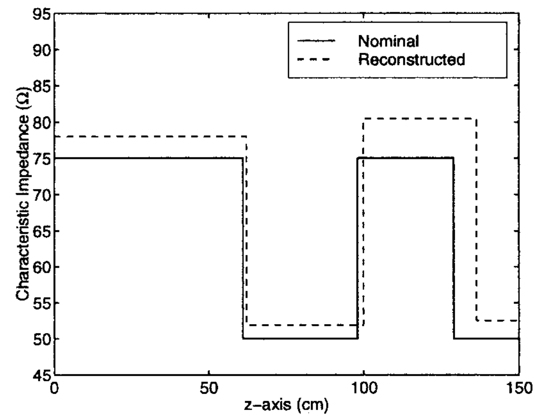

(b)

Fig. 13. A comparison between the known (a) capacitance and (b) characteristic impedance with those provided by the inversion method for the transmission line shown in Fig. 10.

of the inversion method can be observed from this example. First, the objective function has several local minima. Consequently, local optimization methods cannot in general find the right solution. Second, the global minimum of the three-layer structure is the same as that of the four-layer structure. For the latter case, the thickness of one layer has converged to zero. The third feature is that both the conductivity and permittivity profiles can be simultaneously reconstructed from the reflection coefficients obtained for normal incidence.

The results in the presence of a Gaussian noise with a standard deviation $\bar{\sigma} = 10^{-3}$ are shown in Figs. 6 and 7, where the influence of the noise is clearly visible. Nevertheless, this influence can be reduced by extending the data to include more frequencies and incident angles. In Fig. 8, the data at 15 frequencies over the range of [5 MHz, 75 MHz] and at two incident angles $\theta = 0°, 45°$ have been used. The improvement is apparent. Further improvement can be achieved by doubling the frequency points (Fig. 9). It should be noted that the number of layers is assumed to be there for the results of Figs. 8 and 9.

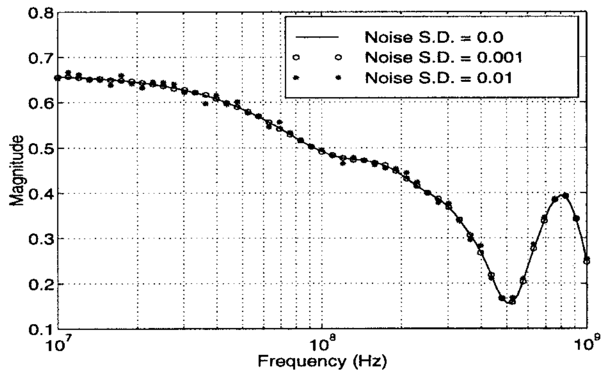

(a)

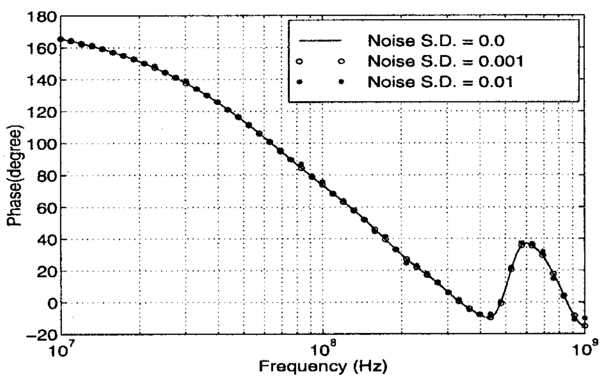

(b)

Fig. 14. Synthetic data for the reflection coefficient of the transmission line whose profile is shown by the solid lines in Fig. 16. The data is obtained at 101 frequencies with logarithmic spacing in the interval [10 MHz, 1 GHz].

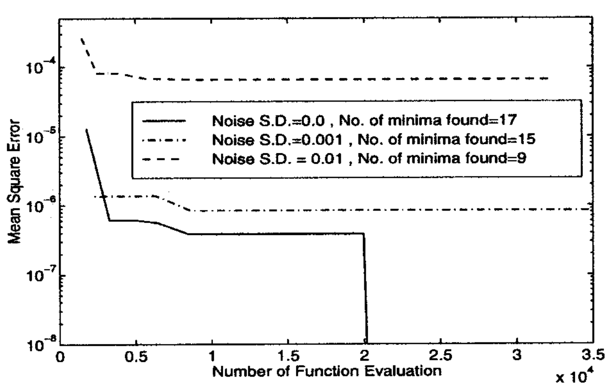

Fig. 15. The objective function versus the number of function evaluation.

Example 2 This example aims at testing the inversion method with experimental data. A nonuniform transmission line which consists of four coaxial sections as shown in Fig. 10, is investigated. An HP-8753B network analyzer with an output impedance of 50 Ω is used to measure the reflection coefficients. The lines are standard 50 Ω and 75 Ω coaxial cables which have negligible series resistance and shunt conductance. The nominal value of the shunt capacitance per unit length C_m, provided by the manufacturer, is 100 pF/m for 50 Ω line and 56 pF/m for 75 Ω line. The series inductance L_m (given in Fig. 10) is calculated by using

$$Z_m = (L_m/C_m)^{1/2} \tag{32}$$

where Z_m is the characteristic impedance of the mth section. The fourth line is terminated by a 50-Ω load so that it can be considered as an infinitely long transmission line.

Since the value of R_m and G_m of the lines are nearly zero, the value of one of the three parameters L_m, C_m, and h_m has to be known according to the necessary condition. In this example, the value of L_m is assumed known and C_m and h_m are reconstructed by the inversion method. The bounds of these parameters are set to

$$\begin{aligned}&35.3 \le C_1, C_3 \le 200 \text{ pF/m}, \quad 44.5 \le C_2, C_4 \le 200 \text{ pF/m}\\ &0 \le h_1, h_2, h_3 \le 200 \text{ cm}.\end{aligned}$$

The lower bounds of C_m are obtained in accordance with $(L_m C_m)^{-1/2} \le 3 \times 10^8$ m/s which indicates the velocity of the wave traveling along the lines cannot be in excess of the velocity of light. The parameters of P and ξ in the MLSL method are set to 100 and 0.05, respectively.

The reflection coefficients measured at 16 frequencies over the frequency range of [100 MHz, 250 MHz] with linear spacing are shown in Fig. 11. The objective function during minimization and the reconstructed profile are illustrated in Figs. 12 and 13, respectively. The profile of the characteristic impedance shown in Fig. 13(b) is obtained from the profile of the capacitance per unit length by using (32). Note that in this example the number of sections is assumed to be four. It can be seen that there is an error in the reconstructed profile. Although the measurement noise can be considered having contributed in generating this error, we think the dominant sources of this error are the following.

1) The value of the capacitance per unit length is a nominal value and the actual value may be different from the nominal one.
2) The series resistance is neglected whereas its value for 50-Ω cables at 100 MHz is nearly 2 Ω/m which is considerable.

Example 3: This example is concerned with the simultaneous reconstruction of four parameters R, L, G, and C of a nonuniform transmission line from synthetic data assuming that the lengths of the sections are known. In practice, these parameters vary with frequency. The variations of L, G, and C are small whereas that of R is considerable. The frequency dependence of R_m can be modeled by $R_m = Q_m\sqrt{\omega}$. Thus, Q_m is to be reconstructed. Consequently, (24) is replaced with the following expression:

$$\begin{aligned}\frac{\partial Y_m}{\partial Q_m} &= -\sqrt{\omega_n}\frac{Y_m^2}{2u_m}\\ \frac{\partial T_m}{\partial Q_m} &= \sqrt{\omega_n}\frac{Y_m[1-(T_m)^2]h_m}{2}.\end{aligned} \tag{33}$$

The line parameters chosen for this example are shown by the solid lines in Fig. 16. The corresponding values for the parameter Q_m are

$$Q_1 = 0, \quad Q_2 = 2 \times 10^{-4}, \quad Q_3 = 5 \times 10^{-4}, \qquad Q_4 = 0.$$

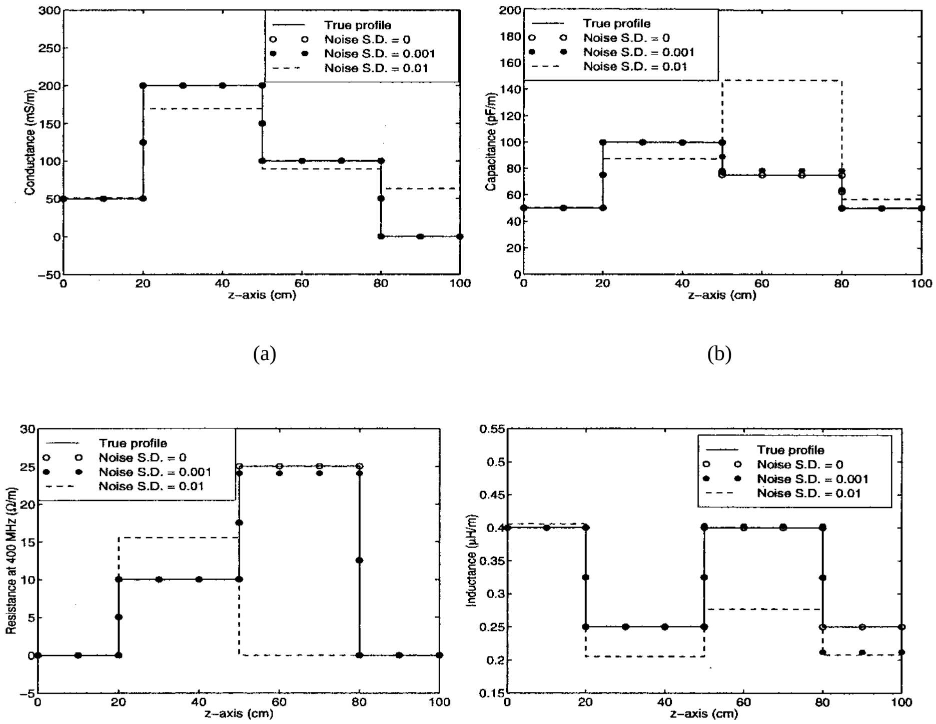

(a) (b)

(c) (d)

Fig. 16. Simultaneous reconstruction of the (a) conductance G, (b) capacitance C, (c) resistance R, and (d) inductance L.

The line is excited from a uniform line with a characteristic admittance $Y_0 = 0.02$ S/m. The other side is left open, i.e., $Y_M = 0$. The parameters of P and ξ in the MLSL method are set to 1000 and 0.005, respectively. The search region is selected as

$$0 \leq Q_m \leq 0.01, \quad 1/(0.09C_m) \leq L_m \leq 0.55\ \mu\text{H/m}$$
$$0 \leq G_m \leq 1000\ \text{mS/m}, \quad 10 \leq C_m \leq 200\ \text{pF/m}, \quad \text{for } m = 1, 2, 3, 4.$$

Figs. 15 and 16 show the objective function graph and the reconstructed profiles which make use of the synthetic data shown in Fig. 14. For the noise-free data, the objective function approached zero and, therefore, the profiles were precisely reconstructed.

V. Conclusion

A one-dimensional inverse scattering method for reconstructing the parameters of layered media and nonuniform transmission lines has been proposed. The method is based on minimizing the MSE between the measured and calculated data using the multilevel single-linkage method. Unlike the inversion methods based on local optimization technique, the proposed method is more likely to converge to the actual profile regardless of the initial one. The gradient of the objective function has been given in a closed form, which greatly improves the efficiency of the MLSL method.

The reconstruction technique has been tested with both synthetic and experimental data. It has been demonstrated that the method is successful with a minimum amount of information regarding the structure of the system under investigation. If the observed data is free from noise, accurate reconstruction can be achieved. When the observed data is corrupted by noise, the adverse effect of noise can be reduced by using an enlarged observed data.

Further improvement in the performance of the reconstruction algorithm in the presence of noise may be achieved by adding an appropriate regularization factor to the MSE function. This is left for future work.

References

[1] M. Sen and P. L. Stoffa, *Global Optimization Methods in Geophysical Inversion*. Amsterdam, The Netherlands: Elsevier, 1995.
[2] A. M. Bruckstein and T. Kailath, "Inverse scattering for discrete transmission-line models," *SIAM Rev.*, vol. 29, no. 3, Sept. 1987.
[3] J. L. Frolik and A. E. Yagle, "Reconstruction of multilayered lossy dielectrics from plane wave impulse responses at two angles of incidence," *IEEE Trans. Geosci. Remote Sensing*, vol. 33, pp. 268–279, Mar. 1995.
[4] J. L. Frolik and A. E. Yagle, "Forward and inverse scattering for discrete layered lossy and absorbing media," *IEEE Trans. Circuits Syst. II*, vol. 44, pp. 710–722, Sept. 1997.
[5] T. Uno and S. Adachi, "Inverse scattering method for one-dimensional inhomogeneous layered media," *IEEE Trans. Antennas Propagat.*, vol. AP-35, pp. 1456–1466, Dec. 1987.
[6] M. Norgren and S. He, "An optimization approach to the frequency-domain inverse problem for a nonuniform LCRG transmission line," *IEEE Trans. Microwave Theory Tech.*, vol. 44, pp. 1503–1507, Aug. 1996.
[7] S. He, P. Fuks, and G. W. Larson, "An optimization approach to time-domain electromagnetic inverse problem for a stratified dispersive and dissipative slab," *IEEE Trans. Antennas Propagat.*, vol. 44, pp. 1277–1282, Sept. 1996.
[8] L. Garnero, A. Franchois, J. Hugonin, C. Pichot, and N. Joachimowicz, "Microwave imaging-complex permittivity reconstruction by

simulated annealing," *IEEE Trans. Microwave Theory Tech.*, vol. 39, pp. 1801–1807, Nov. 1991.

[9] E. Aarts and J. Korst, *Simulated Annealing and Boltzmann Machines*. New York: Wiley, 1989.

[10] Z. Michalewicz, *Genetic Algorithms + Data Structures = Evolution Programs*. New York: Springer-Verlag, 1992.

[11] A. R. Kan and G. Timmer, "Stochastic optimization methods—Part I: Clustering methods," *Mathemat. Prog.*, vol. 39, pp. 27–56, 1987.

[12] A. R. Kan and G. Timmer, "Stochastic optimization methods—Part II: Multilevel methods," *Mathemat. Prog.*, vol. 39, pp. 57–78, 1987.

[13] R. Byrd, C. Dert, A. R. Kan, and R. Schnabel, "Concurrent stochastic methods for global optimization," *Mathemat. Prog.*, vol. 46, pp. 1–29, 1990.

[14] J. M. Renders and S. P. Flasse, "Hybrid methods using genetic algorithms for global optimization," *IEEE Trans. Syst., Man, Cybern.—Part B: Cybern.*, vol. 26, pp. 243–258, Apr. 1996.

[15] M. Nakhkash, "The application of ground penetrating radar to the characterization of multilayered media," Ph.D. dissertation, Univ. Liverpool, U.K., 1999.

[16] J. R. Wait, *Wave Propagation Theory*. New York: Pergamon, 1981.

[17] S. Ramo, J. R. Whinnery, and T. V. Duzer, *Fields and Waves in Communication Electronics*. New York: Wiley, 1994.

[18] L. C. Dixon and G. P. Szego, *Toward Global Optimization 2*. Amsterdam, The Netherlands: North-Holland, 1978.

[19] B. E. Stuckman and E. E. Easom, "A comparison of bayesian/sampling global optimization techniques," *IEEE Trans. Syst., Man, Cybern.*, vol. 22, pp. 1024–1032, Sept./Oct. 1992.

[20] N.A.G., *N.A.G Fortran Library Manual, Mark 16*. Oxford, U.K.: Numerical Algorithm Group, 1996.

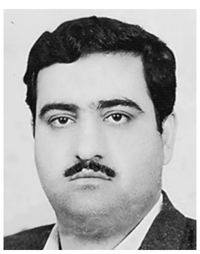

Mansor Nakhkash (M'99) received the B.Sc. and M.Sc. degrees in electrical engineering from Isfahan University of Technology, Isfahan, Iran, in 1988 and 1991, respectively, and the Ph.D. degree in electrical engineering from the University of Liverpool, U.K., in 1999.

He was a Research Staff Member at University of Yazd, Yazd, Iran, from 1991 to 1995, where he worked on several projects related to remote control systems. His current interests include electromagnetic inverse scattering, nondestructive testing, global optimization, computational electromagnetics, and radio communication.

Yi Huang (S'93–A'95–M'96) received the B.Sc. degree in physics from Wuhan University, Wuhan, China, in 1984, the M.Sc. degree in electronic engineering from Nanjing Research Institute of Electronics Technology (NRIET), Nanjing, China, in 1987, and the D.Phil. degree from the University of Oxford, U.K., in 1993.

He spent three years as a Research and Development Engineer at the NRIET, where he was involved in various aspects of the design and development of antennas and microwaves systems. He investigated superconducting antenna arrays at University of Birmingham, U.K., in 1990, and then joined the Department of Engineering Science, University of Oxford, as a Research Associate, where he was engaged in electromagnetic compatibility and nonintrusive probing research. He was a Senior Research Officer in Antennas and Communication at the University of Essex, U.K., and a Visiting Fellow at British Telecom (BT), U.K., in 1994. He has been a Lecturer in Communications and Electromagnetics at the Department of Electrical Engineering and Electronics, University of Liverpool, since 1995. His main research interests are antennas and radio propagation, electromagnetic compatibility and electromagnetic measurements, computational electromagnetics, ground penetrating radar, and indoor wireless communications.

Michael T. C. Fang studied electrical engineering at Tsinghua University, Beijing, China. He received the B.A. degree in electrical sciences from Cambridge University, Cambridge, U.K., in 1965, and the D.Phil. and D.Sc. degrees from Oxford University, Oxford, U.K., in 1969 and 1995, respectively.

He was a Research Fellow at Oxford University (1968–1969), working on plasma waves, and at Imperial College, London, U.K. (1969–1970), working on space plasmas. In 1970, he joined the Department of Electrical Engineering and Electronics, University of Liverpool, where he is Professor of applied electromagnetism. He is a Visiting Professor of Tsinghua University and of Xian Jieotong University in China. He has authored and coauthored more than 140 papers. His current interests are mainly concerned with arc discharges, plasma chemistry, and the applications of artificial intelligence and ground penetration radar for pollution detection.

Dr. Fang is a member of the Current Zero Club and a fellow of the Institution of Electrical Engineers. He served on the Plasma Physics Committee of the Institute of Physics, and on Committee S3 of the Institution of Electrical Engineers in the U.K.